Article

Highly Luminescent, Triple- and Quadruple-Stranded, Dinuclear Eu, Nd, and Sm(III) Lanthanide Complexes Based on Bis-Diketonate Ligands

Andrew P. Bassett, Steven W. Magennis, Peter B. Glover, David J. Lewis, Neil Spencer, Simon Parsons, Ren M. Williams, Luisa De Cola, and Zoe Pikramenou

J. Am. Chem. Soc., **2004**, 126 (30), 9413-9424• DOI: 10.1021/ja048022z • Publication Date (Web): 08 July 2004

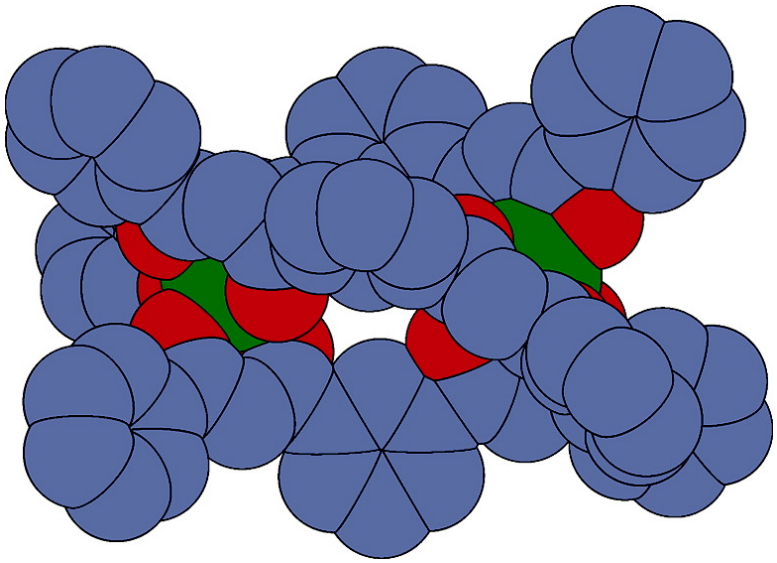

J|A|C|S
ARTICLES
Published on Web 07/08/2004

Highly Luminescent, Triple- and Quadruple-Stranded, Dinuclear Eu, Nd, and Sm(III) Lanthanide Complexes Based on Bis-Diketonate Ligands

Andrew P. Bassett,[†] Steven W. Magennis,[‡] Peter B. Glover,[†] David J. Lewis,[†] Neil Spencer,[†] Simon Parsons,[‡] René M. Williams,[§] Luisa De Cola,[§] and Zoe Pikramenou*,[†]

Contribution from the School of Chemistry, The University of Birmingham, Edgbaston, B15 2TT, United Kingdom, School of Chemistry, The University of Edinburgh, King's Buildings, West Mains Road, Edinburgh, EH9 3JJ, United Kingdom, and Molecular Photonic Materials, Institute of Molecular Chemistry, Faculty of Science, University of Amsterdam, Nieuwe Achtergracht 166, 1018 WS Amsterdam, The Netherlands

Received April 6, 2004; E-mail: z.pikramenou@bham.ac.uk

Abstract: The bis(β-diketone) ligands 1,3-bis(3-phenyl-3-oxopropanoyl)benzene, $H_2\mathbf{L^1}$ and 1,3-bis(3-phenyl-3-oxopropanoyl) 5-ethoxy-benzene, $H_2\mathbf{L^2}$, have been prepared for the examination of dinuclear lanthanide complex formation and investigation of their properties as sensitizers for lanthanide luminescence. The ligands bear two conjugated diketonate binding sites linked by a 1,3-phenylene spacer. The ligands bind to lanthanide(III) or yttrium(III) ions to form neutral homodimetallic triple stranded complexes $[M_2\mathbf{L^1}_3]$ where M = Eu, Nd, Sm, Y, Gd and $[M_2\mathbf{L^2}_3]$, where M = Eu, Nd or anionic quadruple-stranded dinuclear lanthanide units, $[Eu_2\mathbf{L^1}_4]^{2-}$. The crystal structure of the free ligand $H_2\mathbf{L^1}$ has been determined and shows a twisted arrangement of the two binding sites around the 1,3-phenylene spacer. The dinuclear complexes have been isolated and fully characterized. Detailed NMR investigations of the complexes confirm the formation of a single complex species, with high symmetry; the complexes show clear proton patterns with chemical shifts of a wide range due to the lanthanide paramagnetism. Addition of Pirkle's reagent to solutions of the complexes leads to splitting of the peaks, confirming the chiral nature of the complexes. Electrospray and MALDI mass spectrometry have been used to identify complex formulation and characteristic isotope patterns for the different lanthanide complexes have been obtained. The complexes have high molar absorption coefficients (around 13×10^4 $M^{-1}cm^{-1}$) and display strong visible (red or pink) or NIR luminescence upon irradiation at the ligand band around 350 nm, depending on the choice of the lanthanide. Emission quantum yield experiments have been performed and the luminescence signals of the dinuclear complexes have been found to be up to 11 times more intense than the luminescence signals of the mononuclear analogues. The emission quantum yields and the luminescence lifetimes are determined to be 5% and 220 μs for $[Eu_2\mathbf{L^1}_3]$, 0.16% and 13 μs for $[Sm_2\mathbf{L^1}_3]$, and 0.6% and 1.5 μs for $[Nd_2\mathbf{L^1}_3]$. The energy level of the ligand triplet state was determined from the 77 K spectrum of $[Gd_2\mathbf{L^1}_3]$. The bis-diketonate ligand is shown to be an efficient sensitizer, particularly for Sm and Nd. Photophysical studies of the europium complexes at room temperature and 77 K show the presence of a thermally activated deactivation pathway, which we attribute to ligand-to-metal charge transfer (LMCT). Quenching of the luminescence from this level seems to be operational for the Eu(III) complex but not for complexes of Sm(III) and Nd(III), which exhibit long lifetimes. The quadruple-stranded europium complex has been isolated and characterized as the piperidinium salt of $[Eu_2\mathbf{L^1}_4]^{2-}$. Compared with the triple-stranded Eu(III) complex in the solid state, the quadruple-stranded complex displays a more intense emission signal with a distinct emission pattern indicating the higher symmetry of the quadruple-stranded complex.

Introduction

The design of molecular lanthanide complexes with defined architecture is important in order to investigate structure vs properties relationships in lanthanide solid-state framework structures,[1] liquid crystalline materials,[2] sensors[3] or luminescent label design[4] for specific biomolecule interactions. The lack of coordination control around the lanthanide imposes a challenge to the formation of lanthanide supramolecular architectures. Ligand design has been based mainly on structures that encapsulate the lanthanide such as macrocycles and cryptands,[5] podands[6] or shell-type ligands,[7] imposing bulkiness around the metal. In this context, the great majority of lanthanide complexes

[†] School of Chemistry, The University of Birmingham.
[‡] School of Chemistry, The University of Edinburgh.
[§] Molecular Photonic Materials, Institute of Molecular Chemistry, Faculty of Science, University of Amsterdam.

10.1021/ja048022z CCC: $27.50

studied are monometallic. There are few reports of macrocyclic ligand preorganization for recognition of two lanthanide ions.[8] The breakthrough in bimetallic lanthanide assembly came with the formation of dinuclear lanthanide helicates based on benzimidazole pyridyl ligands.[9]

We have been interested in employing self-assembly strategies for lanthanide complexes,[4] and have recently used β-diketonates as sensitizers for lanthanide luminescence.[10] Diketonate ligands have the advantage of a negatively charged binding site that leads to neutral, 3:1 ligand:lanthanide luminescent complexes.[11] The complexes are stable in aqueous solutions and indeed lanthanide diketonate complexes have found many applications from chiral sensing[12] to antibody labels in DELFIA immunoassays,[13] and more recently in the development of new materials based on sol−gel glasses,[14] liquid crystals,[15] near-IR LEDs[16] or polymers.[17] One approach to increase the luminescence output signal is to introduce ligands with multiple binding sites. We have therefore chosen to examine a bis-(β-diketonate) ligand for the formation of dinuclear lanthanide complexes and report our studies on such systems herein.

Scheme 1. Structures of the Dinucleating Ligands, H_2L^1 and H_2L^2

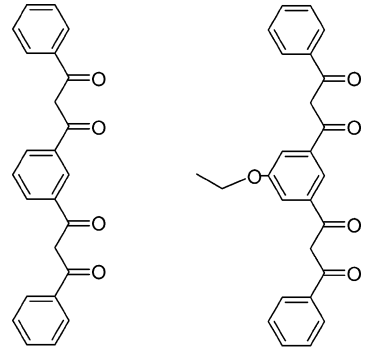

H_2L^1 **H_2L^2**

Ligand $H_2\mathbf{L^1}$ bears two benzoyl β-diketonate sites joined by a 1,3-phenylene spacer unit (Scheme 1). The 1,3-phenylene spacer is ideal for formation of helicate metal complexes.[18] Indeed, this ligand has been shown to form triple helical complexes with Ti(III), V(III), Mn(III), and Fe(III)[19] and a modified ligand has been reported recently to lead to trinuclear triple stranded helical Mn(II) complexes.[20] Dinuclear lanthanide diketonate complexes have received scant attention, with an exception of a recent report during the course of this work.[21] We report herein our studies to fully characterize $H_2\mathbf{L^1}$, determine the formation of dinuclear lanthanide complexes of $H_2\mathbf{L^1}$ and its properties as a sensitizer ligand for lanthanide ions. The Eu(III), Sm(III) and Nd(III) complexes of $H_2\mathbf{L^1}$ are reported. To determine the helical nature of the complexes we extended our approach to synthesize $H_2\mathbf{L^2}$, a derivative of $H_2\mathbf{L^1}$ with an ethoxy substituent as a handle for NMR spectroscopic investigation in the characterization of the lanthanide complexes. A quadruple-stranded dinuclear europium complex of $H_2\mathbf{L^1}$ is also reported herein, which displays strong luminescence signal with a pattern distinct from that of the triple stranded europium complex.

Experimental Section

Materials and Methods. Starting materials were of reagent grade and used without further purification, unless otherwise stated. Solvents were of HPLC grade. $LnCl_3 \cdot 6H_2O$ Ln = Eu, Sm, Nd, and $YCl_3 \cdot 6H_2O$ were obtained from Aldrich (99.9%); acetophenone from BDH, dimethyl isophthalate from Acros, NaH as 60% dispersion in mineral oil from Aldrich (washed several times with hexane to remove oil). Spectroscopic grade DMF (Aldrich) and deuterated solvents (Goss Scientific) were used as received. Anhydrous THF and acetonitrile were freshly distilled over sodium-benzopheneone and P_2O_5, respectively, under dinitrogen. Ligand synthesis was performed under dinitrogen using standard Schlenk and vacuum line techniques. Subsequent workup of products was carried out without precautions to exclude air.

^{1}H- and ^{13}C{^{1}H} NMR spectra were recorded on Bruker AC-300, 360, 500 MHz spectrometers. ^{1}H and ^{13}C{^{1}H} shifts were referenced to external $SiMe_4$. Positive ion FAB and MALDI-TOF mass spectra

(1) Pan, L.; Adams, K. M.; Hernandez, H. E.; Wang, X. T.; Zheng, C.; Hattori, Y.; Kaneko, K. *J. Am. Chem. Soc.* **2003**, *125*, 3062; Klonkowski, A. M.; Lis, S.; Pietraszkiewicz, M.; Hnatejko, Z.; Czarnobaj, K.; Elbanowski, M. *Chem. Mater.* **2003**, *15*, 656; Piggot, P. M. T.; Hall, L. A.; White, A. J. P.; Williams, D. J. *Inorg. Chem.* **2003**, *42*, 8344; Thirumurugan, A.; Pati, S. K.; Green, M. A.; Natarajan, S. *J. Mater. Chem.* **2003**, *13*, 2937; Thompson, D. S.; Thompson, D. W.; Southward, R. E. *Chem. Mater.* **2002**, *14*, 30; Shi, J. M.; Xu, W.; Liu, Q. Y.; Liu, F. L.; Huang, Z. L.; Lei, H.; Yu, W. T.; Fang, Q. *Chem. Commun.* **2002**, 756; Long, D. L.; Blake, A. J.; Champness, N. R.; Wilson, C.; Schroder, M. *Angew. Chem., Int. Ed.* **2001**, *40*, 2444.

(2) Binnemans, K.; Goerller-Walrand, C. *Chem. Rev.* **2002**, *102*, 2302; Nozary, H.; Piguet, C.; Rivera, J. P.; Tissot, P.; Morgantini, P. Y.; Weber, J.; Bernardinelli, G.; Bunzli, J. C. G.; Deschenaux, R.; Donnio, B.; Guillon, D. *Chem. Mater.* **2002**, *14*, 1075.

(3) Rudzinski, C. M.; Young, A. M.; Nocera, D. G. *J. Am. Chem. Soc.* **2002**, *124*, 1723; Parker, D. *Coord. Chem. Rev.* **2000**, *205*, 109.

(4) Glover, P. B.; Rodger, A.; Ashton, P. R.; Kercher, M.; Williams, R. M.; De Cola, L.; Pikramenou, Z. *J. Am. Chem. Soc.* **2003**, *125*, 9918; Charbonniere, L.; Ziessel, R.; Guardigli, M.; Roda, A.; Sabbatini, N.; Cesario, M. *J. Am. Chem. Soc.* **2001**, *123*, 2436; Vazquez-Ibar, J. L.; Weinglass, A. B.; Kaback, H. R. *Proc. Natl. Acad. Sci. U.S.A.* **2002**, *99*, 3487; Bobba, G.; Kean, S. D.; Parker, D.; Beeby, A.; Baker, G. *Perkin Trans. 2* **2001**, 1738; Horrocks, W. D.; Bolender, J. P.; Smith, W. D.; Supkowski, R. M. *J. Am. Chem. Soc.* **1997**, *119*, 5972.

(5) Parker, D.; Dickins, R. S.; Puschmann, H.; Crossland, C.; Howard, J. A. K. *Chem. Rev.* **2002**, *102*, 1977; Zucchi, G.; Ferrand, A. C.; Scopelliti, R.; Bunzli, J. C. G. *Inorg. Chem.* **2002**, *41*, 2459; Gawryszewska, P.; Jerzykiewicz, L.; Pietraszkiewicz, M.; Legendziewicz, J.; Riehl, J. P. *Inorg. Chem.* **2000**, *39*, 5365; Balzani, V.; Scandola, F. In *Comprehensive Supramolecular Chemistry*; Elselvier Science,: Oxford, UK, 1996; Vol. 10, pp 687; Sabbatini, N.; Guardigli, M.; Lehn, J.-M. *Coord. Chem. Rev.* **1993**, *123*, 201.

(6) Marques, N.; Sella, A.; Takats, J. *Chem. Rev.* **2002**, *102*, 2137; Charbonniere, L. J.; Ziessel, R. *Helv. Chim. Acta* **2003**, *86*, 3402; Motson, G. R.; Mamula, O.; Jeffery, J. C.; McCleverty, J. A.; Ward, M. D.; von Zelewsky, A. *J. Chem. Soc., Dalton Trans.* **2001**, 1389; Bretonnière, Y.; Wietzke, R.; Lebrun, C.; Mazzanti, M.; Pécaut, J. *Inorg. Chem.* **2000**, *39*, 3499; Lessmann, J. J.; DeW. Horrocks, W. J. *Inorg. Chem.* **2000**, *39*, 3114.

(7) Magennis, S. W.; Parsons, S.; Pikramenou, Z. *Chem. Eur. J.* **2002**, *8*, 5761; Lowe, M. P.; Caravan, P.; Rettig, S. J.; Orvig, C. *Inorg. Chem.* **1998**, *37*, 1637.

(8) Setyawati, I. A.; Liu, S.; Rettig, S. J.; Orvig, C. *Inorg. Chem.* **2000**, *39*, 496; Avecilla, F.; de Blas, A.; Bastida, R.; Fenton, D. E.; Mahía, J.; Macías, A.; Platas, C.; Rodríguez, A.; Rodríguez-Blas, T. *Chem. Commun.* **1999**, 125; Ziessel, R.; Maestri, M.; Prodi, L.; Balzani, V.; Van Dorsselaer, A. *Inorg. Chem.* **1993**, *32*, 1237.

(9) Bunzli, J.-C. G.; Piguet, C. *Chem. Rev.* **2002**, *102*, 1897.

(10) Magennis, S. W.; Craig, J.; Gardner, A.; Fucassi, F.; Cragg, P. J.; Robertson, N.; Parsons, S.; Pikramenou, Z. *Polyhedron* **2003**, 745.

(11) Weissman, S. I. *J. Chem. Phys.* **1942**, *10*, 214.

(12) Tsukube, H.; Shinoda, S. *Chem. Rev.* **2002**, *102*, 2389.

(13) Hemmilä, I. A. *Applications of Fluorescence in Immunoassays*; J. Wiley & Sons: New York, 1991; Vol. 117 Chemical Analysis Series.

(14) Binnemans, K.; Lenaerts, P.; Driesen, K.; Gorller-Walrand, C. *J. Mater. Chem.* **2004**, *14*, 191.

(15) Van Deun, R.; Moors, D.; De Fre, B.; Binnemans, K. *J. Mater. Chem.* **2003**, *13*, 1520.

(16) Kang, T.-S.; Harrison, B. S.; Bouguettaya, M.; Foley, T. J.; Boncella, J. M.; Schanze, K. S.; Reynolds, J. R. *Adv. Funct. Mater.* **2003**, *13*, 205.

(17) Bender, J. L.; Corbin, P. S.; Fraser, C. L.; Metcalf, D. H.; Richardson, F. S.; Thomas, E. L.; Urbas, A. M. *J. Am. Chem. Soc.* **2002**, *124*, 8526.

(18) Constable, E. C.; Hannon, M. J.; Tocher, D. A. *J. Chem. Soc., Dalton Trans.* **1993**, 1883; Dietrich-Buchecker, C.; Rapenne, G.; Sauvage, J. P.; De Cian, A.; Fischer, J. *Chem. Eur. J.* **1999**, *5*, 1432.

(19) Grillo, V. A.; Seddon, E. J.; Grant, C. M.; Aromí, G.; Bollinger, J. C.; Folting, K.; Christou, G. *Chem. Commun.* **1997**, 1561.

(20) AromI, G.; Berzal, P. C.; Gamez, P.; Roubeau, O.; Kooijman, H.; Spek, A. L.; Driessen, W. L.; Reedijk, J. *Angew. Chem., Int. Ed.* **2001**, *40*, 3444.

(21) Yuan, J.; Sueda, S.; Somazawa, R.; Matsumoto, K.; Matsumoto, K. *Chem. Lett.* **2003**, *32*, 492.

were recorded on Kratos MS-50 and Kratos III mass spectrometers, respectively. Elemental analyses were performed using a Perkin-Elmer 2400 CHN elemental analyzer. UV absorption spectra for luminescence studies were recorded on Perkin-Elmer Lambda 9 and Lambda 17 spectrometers. All measurements were made at room temperature (ca. 20 °C) in aerated solutions, unless otherwise stated. Luminescence emission and excitation spectra for Eu(III) and Sm(III) were recorded on a Photon Technology International (PTI) QM-1 emission spectrometer.[22] Emission spectra were corrected for photomultiplier tube response. Lifetime measurements were carried out using a nanosecond Nd:YAG laser (Continuum, Surelite II) as the excitation source in an experimental setup previously described.[7a] The obtained, unweighted, data were analyzed by a nonlinear, least-squares, iterative technique (Marquardt−Levenberg algorithm) using Kaleidagraph software. The luminescence decay curves were fitted to a single exponential of the form $I(t) = I(0)\exp(-t/\tau)$, where $I(t)$ is the intensity at time t after the excitation flash, $I(0)$ is the initial intensity at $t = 0$ and τ is the luminescence lifetime. High Pearson's correlation coefficients (≥ 0.999) were observed in all cases. Lifetimes were reproducible to ± 5%. Luminescence quantum yields for Eu(III) and Sm(III) complexes were measured by an optically dilute relative method[23] using [Ru(2,2′-bipyridyl)$_3$]Cl$_2$ ($\Phi = 0.028$ in aerated H_2O)[24] as a standard. The NIR emission spectra were recorded on a PTI Alphascan fluorimeter, in which a 75 W quartz-tungsten−halogen lamp is focused through a SPEX 1680 double grating monochromator onto the sample. The excitation light was modulated by a mechanical chopper at 35−70 Hz. The emission was detected under a right angle through a 830 nm cutoff filter using a single grating monochromator. A North Coast EO 817L (250 V) liquid nitrogen cooled germanium detector was used, connected to a Stanford Research SR 530 Lock-in-Amplifier. The lifetimes of NIR emission were determined using an Edinburgh instruments LP 900, consisting of a 337 nm nitrogen laser (Laser Technik Berlin, MSG405-TD with pulses of 20 μJ, 0.5 ns fwhm), an Edinburgh Instruments single grating monochromator and a North Coast EO 817P liquid nitrogen cooled germanium detector. The signal was recorded with a Tektronix digitizing oscilloscope, which was triggered by the laser.

Synthesis of 1,3-bis(3-phenyl-3-oxopropanoyl)benzene, H_2L^1. A

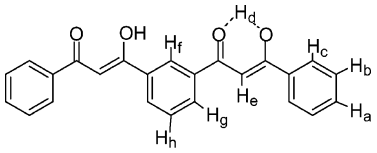

H_2L^1

solution of dimethyl isophthalate (3.27 g, 0.017 mol) and acetophenone (5 g, 0.083 mol) in THF (50 cm^3) was added to NaH (2.0 g, 0.05 mol) at 0−5 °C forming an orange precipitate. The mixture was stirred at this temperature for 2 h and for a further 2 h at room temperature. The NaH was quenched with water and the mixture filtered. Addition of dilute HCl to the yellow/orange solution yielded a pale yellow solid, which was identified as the desired product (2.3 g, 37%).

δ_H (300 MHz, $CDCl_3$): 15.2 (2H, br s, H_d), 8.58 (1H, t, $^4J = 2$ Hz, H_f), 8.17 (2H, dd, $^{3,4}J = 8$, 2 Hz, H_g), 8.01−8.04 (4H, m, H_c), 7.49−7.66 (7H, m, H_a, H_b, H_h), 6.94 (2H, s, H_e); δ_H (300 MHz, d^7-DMF): 15.3 (br s, H_d), 8.92 (1H, t, $^4J = 2$ Hz, H_f), 8.50 (2H, dd, $^{3,4}J = 8$, 2 Hz, H_g), 8.26−8.29 (4H, m, H_c), 7.82 (1H, t, H_h), 7.60−7.74 (8H, m, H_a, H_b, H_e); δ_C {^{1}H} (75 MHz, $CDCl_3$): 186.1, 184.8, 136.2, 135.2, 132.7, 130.7, 129.1, 128.7, 127.3, 125.8, 93.4; FAB-MS *m*/*z* 371[*M* + H]$^+$, 266 [*M* − *COPh*]$^+$; λ_{max}/nm (DMF) 357 ($\epsilon = 4 \times 10^4$ dm^3·mol^{-1}·cm^{-1}); $C_{24}H_{18}O_4$ found: C, 77.7; H, 4.9%, requires C, 77.8; H, 4.9%. Crystallographic data for $\mathbf{H_2L^1}$: $C_{24}H_{18}O_4$, M = 370.38, orthorhombic, space group $P2_12_12_1$, $a = 5.2013(5)$, $b = 16.6336(15)$, $c = 20.8923(18)$ Å, $V = 1807.5(3)$ Å^3, $Z = 4$, $\rho_{calcd} = 1.361$ g cm^{-3}, $F(000) = 776$, synchrotron radiation ($\lambda = 0.68750$ Å), $T = 160$ K, $\mu = 0.092$ mm^{-1}, $R_1 = 0.0793$ [$\theta_{max} = 27°$, 2798 data $F > 4\sigma(F)$], $wR_2 = 0.2499$ for 3580 independent reflections, GOF = 1.102.

General Synthetic Method for $Y_2L^1_3$ and $Ln_2L^1_3$ where Ln = Eu, Sm, Nd, Gd. A solution of $LnCl_3 \cdot 6H_2O$ or $YCl_3 \cdot 6H_2O$ (0.17 mmol) in MeOH (2 cm^3) was added dropwise to a solution of $\mathbf{H_2L^1}$ (0.0915 g, 0.25 mmol) in $CHCl_3$ (8 cm^3), resulting in a pale yellow solution. A solution of NEt_3 (0.052 g, 0.51 mmol) in MeOH (2 cm^3) was added dropwise to this solution, producing a deeper yellow color. A pale yellow precipitate formed after a few seconds. The mixture was stirred for 1 h, filtered, and washed with $CHCl_3$ (2 × 2 cm^3), methanol (4 × 2 cm^3), H_2O (2 × 2 cm^3) and ether (2 × 2 cm^3) and dried under vacuum to give the desired product (yields 55−60%).

[$Y_2\mathbf{L^1}_3$] δ_H (300 MHz, DMF-d_7): 9.64 (3H, H_f), 8.40 (6H, dd, $^{3,4}J = 8$, 2 Hz, H_g), 8.27 (12H, dd, $^{3,4}J = 8$, 2 Hz, H_c), 7.47−7.55 (21H, m, H_a, H_b, H_h), 7.16 (6H, s, H_e); δ_C {^{1}H}: (90.6 MHz, DMF-d_7) 184.5 (CO), 183.5 (CO), 140.5, 140.1, 131.4, 130.5, 128.6, 128.4, 128.1, 127.9, 94.3; FAB−MS *m*/*z* 1283 [*M* + H]$^+$; λ_{max}/nm (DMF) 357 ($\epsilon = 13 \times 10^4$ dm^3·mol^{-1}·cm^{-1}). (Found: C, 67.6; H, 3.9%. $Y_2C_{72}H_{48}O_{12}$ requires: C, 67.4; H, 3.8%).

[$Eu_2\mathbf{L^1}_3$] δ_H (500 MHz, DMF-d_7): 6.5 (6H, t, $^3J = 6.75$ Hz, H_a), 6.4 (15H, br, H_b, H_f), 6.3 (3H, t, $^3J = 6.24$ Hz, H_h), 6.2 (6H, d, $^3J = 6.24$ Hz, H_g), 4.6 (12H, br, H_c), 3.8 (6H, s, H_e); FAB-MS *m*/*z* 1409 [*M* + H]$^+$; λ_{max}/nm (DMF) 357 ($\epsilon = 13 \times 10^4$ dm^3·mol^{-1}·cm^{-1}). (Found: C, 60.7; H, 3.31%. $C_{72}H_{48}O_{12}Eu_2 \cdot H_2O$ requires C, 60.6; H, 3.53%).

[$Sm_2\mathbf{L^1}_3$] δ_H (300 MHz, DMF-d_7): 8.53−8.51 (12H, m, H_c), 8.4 (6H, d, $^3J = 7$ Hz, H_g), 7.9 (6H, s, H_e), 7.56−7.50 (21H, m, H_a, H_b, H_f), 6.75 (3H, br, H_h); MALDI−MS *m*/*z* 1407 [*M* + H]$^+$, 1429 [*M* + Na]$^+$; λ_{max}/nm (DMF) 357 ($\epsilon = 13 \times 10^4$ dm^3·mol^{-1}·cm^{-1}); (Found: C, 61.3; H, 3.2%. $C_{72}H_{48}O_{12}Sm_2$ requires C, 61.5; H, 3.4%).

[$Nd_2\mathbf{L^1}_3$] δ_H (300 MHz, DMF-d_7): 12.0 (18H, m, H_c, H_e), 10.0 (6H, d, $^3J = 7.5$ Hz, H_g), 8.46−8.53 (21H, m, H_a, H_b, H_f), 8.28 (3H, t, $^3J = 7.5$ Hz, H_h); MALDI−MS *m*/*z* 1393 [*M* + H]$^+$, 1415 [*M* + Na]$^+$; λ_{max}/nm (DMF) 357 ($\epsilon = 13 \times 10^4$ dm^3·mol^{-1}·cm^{-1}); (Found: C, 62.0; H, 3.6%. $C_{72}H_{48}O_{12}Nd_2$ requires C, 62.1; H, 3.5%).

[$Gd_2\mathbf{L^1}_3$] MALDI−MS *m*/*z* 1421 [*M* + H]$^+$ 1443 [*M* + Na]$^+$;, Found: C, 61.0; H, 3.2%. $C_{72}H_{48}O_{12}Gd_2$ requires C, 60.9; H, 3.4%.

Synthesis of $(Hpip)_2[Eu_2\mathbf{L^1}_4]$. A solution of $EuCl_3 \cdot 6H_2O$ (0.020 g, 0.055 mmol) in MeOH (6 cm^3) was added dropwise to a solution of $\mathbf{H_2L^1}$ (0.041 g, 0.11 mmol) in $CHCl_3$ (20 cm^3), giving a pale yellow solution. An excess amount of piperidine (pip) was added to this solution, resulting in the immediate formation of a pale yellow precipitate, which was filtered and dried under vacuum.

Found: C, 65.1; H, 4.4; N, 1.3%. $C_{106}H_{88}O_{16}N_2Eu_2$ requires C, 65.3; H, 4.6; N, 1.4%).

ESI−MS(−) *m*/*z* 888 [M-2(Hpip)]$^{2-}$, 1799 [M-2(Hpip) + Na]$^-$, 1777 [M-2(Hpip) + H]$^-$.

Synthesis of dimethyl 5-ethoxyisophthalate

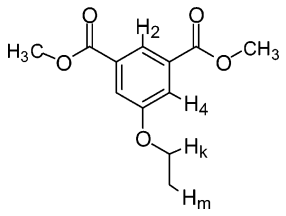

Bromoethane (1.04 g, 1.48 cm^3, 9.52 mmol), was added to a solution of dimethyl 5-hydoxyisophthalate (2.00 g, 9.52 mmol), K_2CO_3 (0.638 g, 4.76 mmol) and tetrabutylammonium chloride (20 mg), in acetonitrile (120 cm^3). The solution was refluxed for 24 h under N_2, to yield an off-white precipitate. The solvent was removed and the product extracted with the following: $CHCl_3$ (100 cm^3), and H_2O (100 cm^3).

(22) Haider, J. M.; Chavarot, M.; Weidner, S.; Sadler, I.; Williams, R. M.; De Cola, L.; Pikramenou, Z. *Inorg. Chem.* **2001**, *40*, 3912.
(23) Demas, J. N.; Crosby, G. A. *J. Phys. Chem.* **1971**, *75*, 991.
(24) Nakamura, K. *Bull. Chem. Soc. Jpn.* **1982**, *55*, 2697.

The organic layer was evaporated to produce a white solid, which was washed with MeOH (2 × 2 cm^3), H_2O (2 × 2 cm^3) and diethyl ether (2 × 2 cm^3), to yield the desired product (2.14 g, 95%) as a white crystalline solid.

δ_H (300 MHz, $CDCl_3$); 8.26 (1H, t, ^4J = 2 Hz, H_2), 7.74 (2H, d, ^4J = 2 Hz, H_4), 4.12 (2H, q, ^3J = 7 Hz, H_k), 3.93 (6H, s, CH_3), 1.44 (3H, t, ^3J = 7 Hz, H_m). $\delta_C\{^1H\}$ (75 MHz, $CDCl_3$); 166.2, 159.0, 131.7, 122.8, 120.8, 119.8, 64.1, 52.4, 14.6. ES+ MS *m*/*z* 261 $[M + Na]^+$

Synthesis of 1,3-bis(3-phenyl-3-oxopropanoyl) 5-ethoxy benzene, H_2L^2

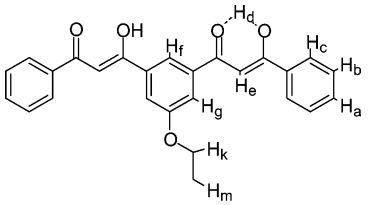

H_2L^2

A solution of dimethyl 5-ethoxyisophthalate (2.00 g, 8.4 mmol) and acetophenone (2.22 g, 2.2 mL, 18 mmol) in THF (30 cm^3) was added to NaH (0.5 g, 21 mmol) at 0−5 °C. The mixture was stirred at this temperature for 2 h and for a further 2 h at room temperature. The remaining unreacted NaH was quenched with water (5 cm^3) and the mixture filtered. Acidification with dilute HCl (8 cm^3, 2 mol dm^{-3}) turned the solution a yellow/orange color. The solvent was completely removed under vacuum and the product extracted using $CHCl_3/H_2O$. The organic layer was reduced in volume to yield a dark brown oil, which was dissolved in the minimum amount of EtOH. To this, hexane was added dropwise, causing a light orange precipitate to form. This was filtered and washed with ice-cold EtOH (2 × 2 cm^3), hexane (2 × 4 cm^3), and diethyl ether (2 × 2 cm^3). The desired product was isolated as a light yellow powder (1.19 g, 34%).

δ_H (300 MHz, $CDCl_3$): 15.3 (br s, H_d), 8.13 (1H, t, ^4J = 2 Hz, H_f), 8.02 (4H, dd, ^4J = 1 Hz, ^3J = 7 Hz, Hc), 7.68 (2H, d, ^4J = 2 Hz, H_g), 7.48−7.61 (6H, m, H_a, H_b), 6.90 (2H, s, H_e), 4.19 (2H, q, ^3J = 7 Hz, H_k), 1.49 (3H, t, ^3J = 7 Hz, H_m); δ_H (300 MHz, DMF-d_7): 15.2 (br s, H_d), 8.53 (1H, t, ^4J = 1.5 Hz, H_f), 8.26−8.29 (4H, m, H_c), 7.97 (2H, d, ^4J = 1.5 Hz, H_g), 7.68−7.73 (2H, m, H_a), 7.58−7.64 (6H, m, H_b, H_e), 4.30 (2H, q, ^3J = 6.9 Hz, H_k), 1.45 (3H, t, ^3J = 6.9 Hz, H_m); $\delta_C\{^1H\}$ (75 MHz, $CDCl_3$): 185.7, 185.0, 159.5, 137.5, 135.2, 132.7, 128.7, 127.2, 118.1, 116.8, 93.5, 64.2, 14.7; ES−MS (+) *m*/*z* 437 $[M + Na]^+$; λ_{max}/nm (DMF) 360 ($\epsilon = 4 \times 10^4$ dm^3 mol^{-1} cm^{-1}); (Found: C, 75.63; H, 5.41%. $C_{26}H_{22}O_5$ requires C, 75.34; H, 5.35%).

General Synthetic Method for $[Ln_2L^2_3]$, where Ln = Eu, Nd. A solution of $LnCl_3 \cdot 6H_2O$ (0.26 mmol) in MeOH (4 cm^3) was added dropwise to a solution of H_2L^2 (0.166 g, 0.40 mmol) in $CHCl_3$ (16 cm^3), resulting in a pale yellow solution. A solution of NEt_3 (0.084 g, 0.82 mmol) in MeOH (4 cm^3) was added dropwise to this solution, producing a deeper yellow color. A pale yellow precipitate formed after a few minutes. The mixture was stirred for 2 h, filtered, and washed with $CHCl_3$ (2 × 2 cm^3), methanol (4 × 2 cm^3), H_2O (2 × 2 cm^3) and ether (2 × 2 cm^3) and dried to give the desired product (yields 50−60%).

$[Eu_2L^2_3]$ δ_H (500 MHz, DMF-d_7): 6.5 (6H, t, ^3J = 7.0 Hz, H_a), 6.4 (15H, m, H_b, H_f), 5.6 (6H, s, H_g), 4.5 (12H, br, H_c), 3.7 (2H, s, H_e), 3.5 (6H, q, ^3J = 7.0 Hz, H_k), 0.9 (9H, t, ^3J = 7.0 Hz, H_m); MALDI−MS *m*/*z* 1542 $[M + H]^+$; λ_{max}/nm (DMF) 360 ($\epsilon = 1 \times 10^5$ dm^3·mol^{-1}·cm^{-1}); (Found: C, 60.7; H, 4.0%. $C_{78}H_{60}O_{15}Eu_2$ requires C, 60.7; H, 3.9%).

$[Nd_2L^2_3]$ δ_H (300 MHz, DMF-d_7): 12.0 (18H, m, H_c, H_e), 9.6 (6H, s, H_g), 8.5 (21H, m, H_a, H_b, H_f), 4.9 (6H, q, ^3J = 6.7 Hz, H_k), 1.9 (9H, t, ^3J = 6.7 Hz, H_m); MALDI-MS *m*/*z* 1547 $[M + Na]^+$; λ_{max}/nm (DMF) 358 ($\epsilon = 1.1 \times 10^5$ dm^3·mol^{-1}·cm^{-1}). (Found: C, 61.6; H, 3.9%. $C_{78}H_{60}O_{15}Nd_2$ requires C, 61.6; H, 4.0%).

Results and Discussion

Preparation and Characterization of Ligands. The ligand H_2L^1 was obtained by the Claisen condensation of dimethyl isophthalate and acetophenone following a modification of the reported preparation.[25] In that report, only IR and melting point characterization of H_2L^1 was reported. We have fully characterized H_2L^1 and have prepared a new ligand H_2L^2 based on condensation of dimethyl 5-ethoxyisophthalate with acetophenone. This ligand bears an ethoxy chain at the back of the central phenyl ring to provide a spectroscopic handle for NMR investigation of the chirality of the corresponding metal complexes.

Single crystals of H_2L^1 suitable for X-ray diffraction analysis were grown by slow evaporation of a methanol solution. The

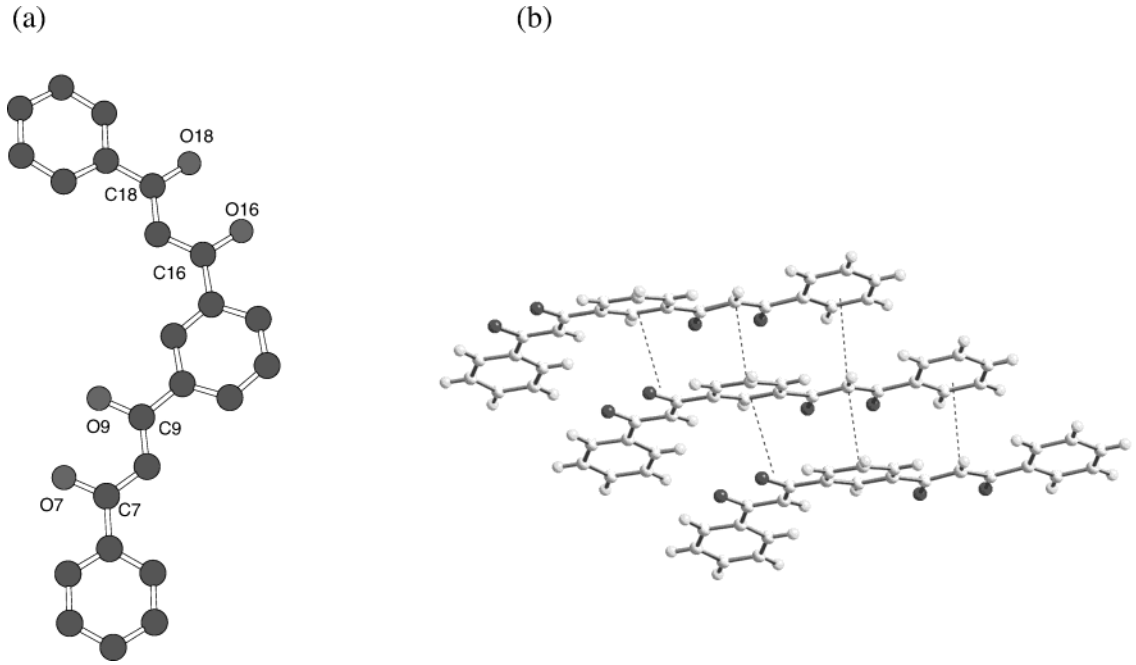

Figure 1. X-ray crystal structure of H_2L^1 showing (a) numbering scheme (b) a stacking arrangement.

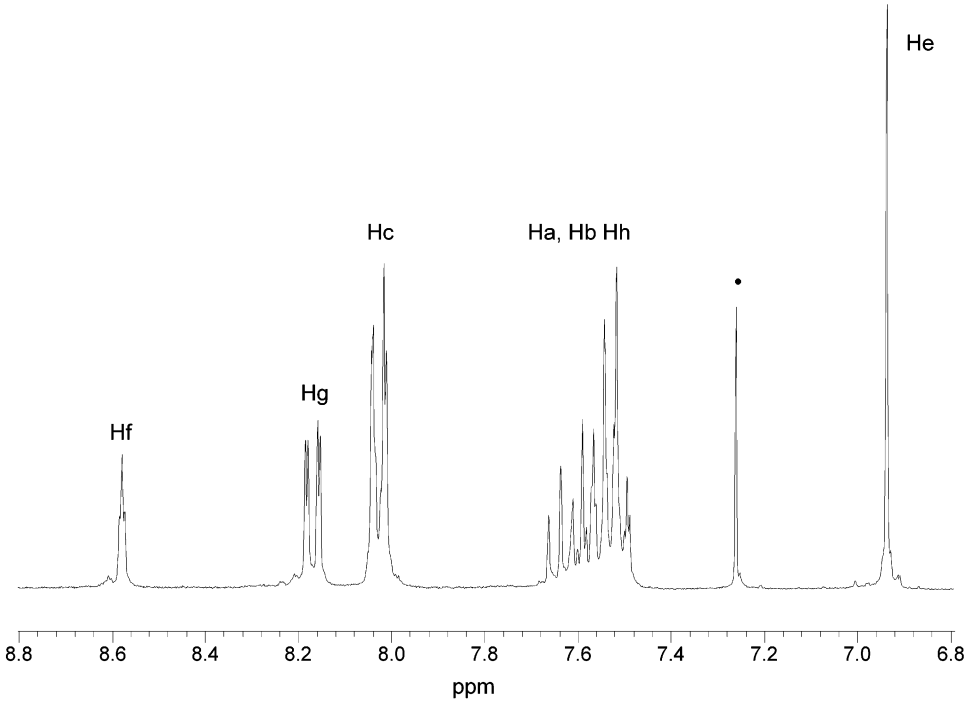

Figure 2. 300 MHz ^{1}H NMR spectrum of $H_2\mathbf{L^1}$ in $CDCl_3$. The dotted peak is due to chloroform.

crystal structure of $H_2\mathbf{L^1}$ (Figure 1 and Supporting Information) shows that the ligand adopts a planar structure as expected to maximize conjugation with the two diketonate units arranged asymmetrically about the 1,3-phenylene spacer, i.e., one diketonate is oriented in the opposite direction from the other, pointing toward different protons around the 1,3-central phenyl ring. The ligands are π-stacked on top of each other to afford columns of ligands with extensive stacking between the central portion of one ligand with the end of an adjacent ligand. In each case, the stacking occurs between a phenyl from one strand and a diketonate from the other. The columns are packed together forming a series of CH$\cdots\pi$ contacts between their terminal phenyl rings which are arranged in a herringbone-type motif.

The bond lengths of this structure can be compared with the reported structure of dibenzoylmethane (HDBM).[26] For $H_2\mathbf{L^1}$, the carbonyl bond lengths for C(7)−O(7) and C(9)−O(9), are of similar value 1.290(4) and 1.297(4), respectively, whereas there is a difference in value of the C(16)−O(16) and C(18)−O(18) bond lengths which are 1.300(5) and 1.283 (5) Å, respectively. These data suggest that in the O(7)/O(9) ring the enolic proton is shared symmetrically with the carbonyl oxygen, whereas in the O(16)/O(18) ring it is not. In HDBM, the C−O bonds are not equidimensional (1.292 and 1.317 Å).[27] The structural data indicate that $H_2\mathbf{L^1}$ exists in the enol form in the solid state.

The ^{1}H NMR spectra of $H_2\mathbf{L^1}$ and $H_2\mathbf{L^2}$ in $CDCl_3$ and d^7-DMF, show the characteristic enolic proton absorptions at around δ 15.2. This is an indication that the enol tautomer for each ligand is the most dominant form in both solvents. In most organic solvents, β-diketones are predominately (> 90%) enolized.[27] In the ^{1}H NMR spectrum of $H_2\mathbf{L^1}$ in $CDCl_3$ (Figure 2) a singlet at δ 6.94 is assigned to the two equivalent methine protons (H_e). The rest of the protons are assigned based on coupling constants and correlations obtained in a ^{1}H−^{1}H COSY spectrum (Supporting Information).

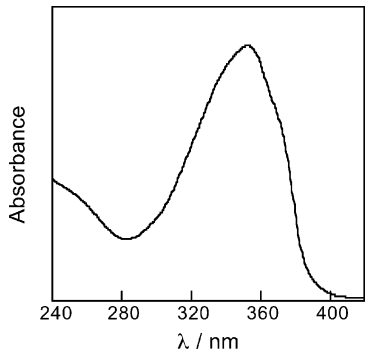

Figure 3. UV−vis absorption spectrum of $H_2\mathbf{L^1}$ in MeOH.

In the ^{1}H NMR spectrum of $H_2\mathbf{L^2}$ (Supporting Information) the only observed differences include the appearances of a quartet and a triplet, assigned to H_k and H_m respectively and the different pattern for H_g and H_c due to the presence of the ethoxy group. The ^{13}C NMR spectra display 11 signals for $H_2\mathbf{L^1}$ and 13 distinct signals for $H_2\mathbf{L^2}$, as expected based on the ligand symmetry (Supporting Information).

The UV−vis absorption spectra of both $H_2\mathbf{L^1}$ (Figure 3) and $H_2\mathbf{L^2}$ exhibited an intense band with $\lambda_{max} = 357$ nm, attributed to singlet−singlet $\pi \rightarrow \pi^*$ enol absorption, characteristic of the enol form of β-diketones.

Synthesis and Characterization of Triple-Stranded Dinuclear Lanthanide Complexes of Bis-Diketonate Ligands $\mathbf{L^1}$ and $\mathbf{L^2}$. Reaction of $H_2\mathbf{L^1}$ or $H_2\mathbf{L^2}$ with a metal chloride hexahydrate in a 3:2 ratio in the presence of triethylamine lead to the formation of $[M_2\mathbf{L^1}_3{\cdot}nH_2O]$, M = Eu, Sm, Nd, Y or $[M_2\mathbf{L^2}_3{\cdot}nH_2O]$, M = Eu, Nd. The solids are soluble in DMF and slightly soluble in alcoholic solvents. Although attempts to grow crystals of the complexes were unsuccessful, NMR and

(25) Martin, D. F.; Shamma, M.; Fernelius, W. C. *J. Am. Chem. Soc.* **1958**, *80*, 4891.
(26) Williams, D. E. *Acta Crystallogr.* **1966**, *21*, 340.
(27) Emsley, J. *Struct. Bonding (Berlin)* **1984**, *57*, 147.

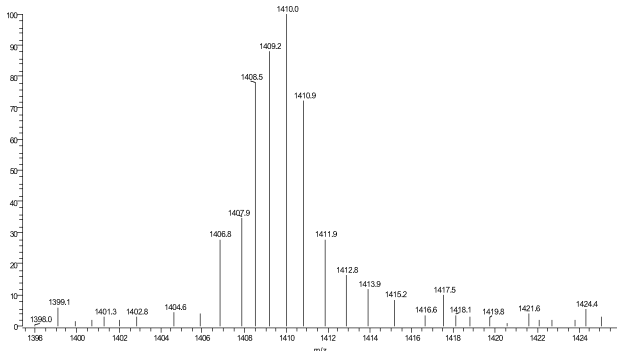

Figure 4. Expanded regions of the ES(+) mass spectrum of $[Eu_2\mathbf{L^1}_3]$ in DMF/CH_3CN.

mass spectrometric analyses were employed and enabled us to identify the molecular species.

Several mass spectrometry ionization methods have been used interchangeably to detect the complexes (Supporting Information). The FAB(+)−MS spectrum of the isolated $[Eu_2\mathbf{L^1}_3]$ product exhibited intense peaks with mass distribution m/z = 1407−1414, corresponding to $[Eu_2\mathbf{L^1}_3 + H]^+$. These peaks in the accurate FAB(+)−MS spectrum of the sample show a pattern in agreement with the theoretical isotope pattern for the dinuclear complex (Supporting Information). Electrospray mass spectrometry provided an insight of the solution formulation of the complex (Figure 4). The peak centered at m/z 1410 is assigned to $[Eu_2\mathbf{L^1}_3 + H]^+$ for the dinuclear complex. MALDI-(+)−S was also used for the complexes. The isotope distributions illustrated in the peaks for the parent ions in all complexes unambiguously confirm the dinuclear formation of the complexes.

NMR spectroscopy was used for the elucidation of complex formation. A clear indication of complex formation of $H_2\mathbf{L^1}$ and $H_2\mathbf{L^2}$ is given by the absence of the enolic proton peak, H_d, present in the free ligands. Spectra of all the complexes show that there is only one species present in solution. The presence of one singlet for the H_e methine protons at δ 7.14 is an indication that the two methine protons on a single ligand are C_2-symmetric and that all three ligands are equivalent. The ^{1}H NMR spectrum of $[Y_2\mathbf{L^1}_3]$ in d_7-DMF is shown in Figure 5. The Y^{3+} ion was chosen as a diamagnetic replacement for Eu^{3+}. The methine protons, H_e, and the aromatic protons H_a, H_b, H_c, H_g, and H_h shift to lower frequencies with respect to their chemical shifts in the d_7-DMF spectrum of the free ligand; most notably, H_e shifts by 0.45 ppm. This shift is consistent with the ligands binding to the metal ion. In contrast, H_f shows a relatively large shift of 0.69 ppm to higher frequency compared to that of the free ligand. This downfield shift was also observed in previously reported dinuclear helical metal complexes bearing a 1,3-phenylene a spacer between the binding units.[18] The $^{13}C\{^1H\}$ NMR spectrum of $[Y_2\mathbf{L^1}_3]$ confirms the complex's high symmetry, showing only 11 distinct resonances (Supporting Information).

The ^{1}H NMR spectra of the complexes of the paramagnetic ions Eu^{3+}, Nd^{3+}, and Sm^{3+} are fully assigned as described below (Figure 6 and Supplementary Info). Although line broadening of certain peaks close to the paramagnetic metal ion was observed, full assignments have been achieved using high-resolution instruments to avoid signal overlap. The shifts due to paramagnetism have their origin in the sum of two contributions: the contact, or *Fermi* shift, δ^c, (which operates through bonds), and the pseudo-contact shift, δ^{pc}, (which operates through space).[28] The pseudo-contact shift is related to the magnetic anisotropy of the complex and the position of the proton in question, with respect to the central paramagnetic ion.[29] Both the distance of the proton from the metal center and the angle between the proton and the main molecular symmetry axis of the molecule are important for the shift variation with

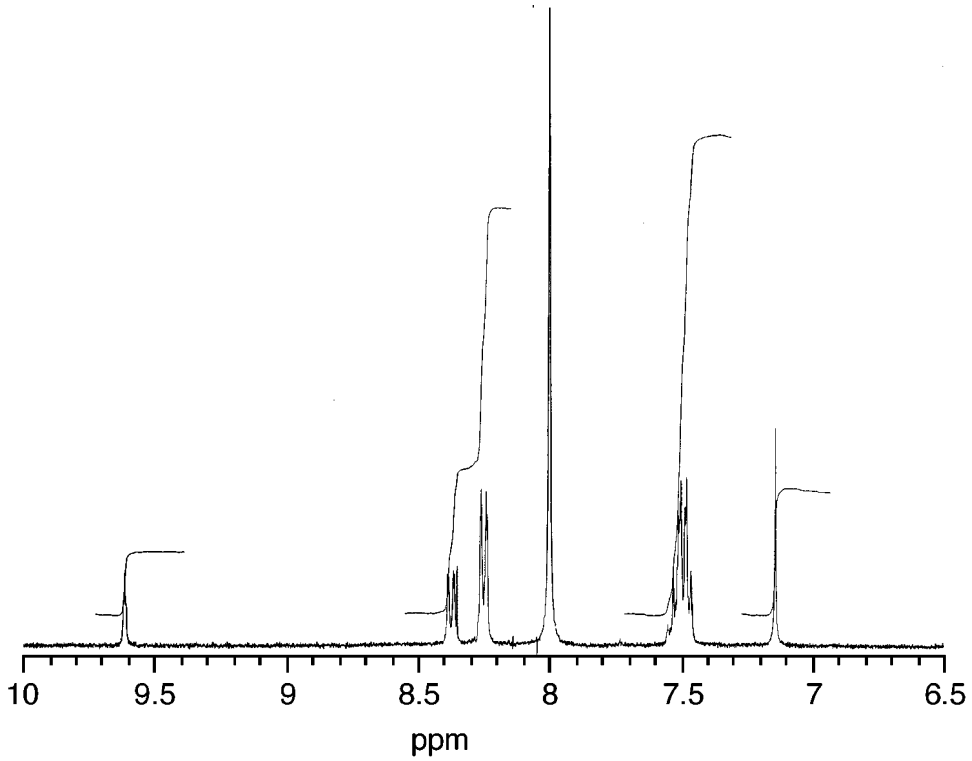

Figure 5. 300 MHz ^{1}H NMR spectrum of $[Y_2\mathbf{L^1}_3]$ in d_7-DMF.

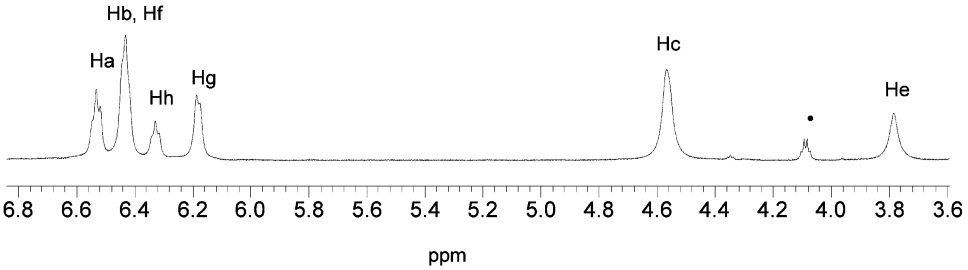

Figure 6. 500 MHz ^{1}H NMR spectrum of [$Eu_2\mathbf{L^1}_3$] in d^7-DMF. The dotted peak is due to the presence of methanol.

the paramagnetic metal ion. The reliance of distance on the observed shift is generally demonstrated in the ^{1}H NMR spectra of the paramagnetic complexes in our case, where protons closer to the metal centers shift by a much larger value in comparison to protons further away. However, the magnitude and sign of the observed shift is also dependent on the angular position of the proton in question which is more difficult to define in the absence of crystal structures. In the following section, the NMR spectra are analyzed in detail in order to elucidate how these assignments have been reached.

The ^{1}H NMR spectrum of [$Eu_2\mathbf{L^1}_3$] (Figure 6) exhibits a triplet at δ 6.53, which integrates for six protons and is assigned as H_a. Protons H_b and H_f appear as an unresolved broad peak at δ 6.43, with the expected integral value. The triplet at δ 6.33 is assigned as H_h and integrates for three protons, its multiplicity arises from coupling to H_g (^3J = 6.24 Hz). H_g appears as a broad doublet at δ 6.18 with a ^3J = 6.24 Hz indicating coupling to H_h, whereas four-bond coupling to H_f is masked by the broadness of the peak. A broad singlet at δ 4.57 is assigned to H_c, integrating for twelve protons. The methine protons, H_e, appear as a broad singlet at δ 3.78 and correctly integrate for six protons. H_e shows the largest shift with respect to the free ligand, as a consequence of the closeness of these protons to the binding site of the ligand and the paramagnetic metal.

The ^{1}H NMR spectrum of [$Eu_2\mathbf{L^2}_3$] in d^7-DMF showed similar chemical shifts and multiplicities for protons H_a, H_b, H_c, H_e, and H_f, as for [$Eu_2\mathbf{L^1}_3$], whereas H_g appears as a singlet, as it no longer couples with the absent H_h. The signals for H_k and H_m appear at δ 3.51 (quartet), and at 0.90 (triplet), respectively. It was anticipated from the design of the $H_2\mathbf{L^2}$ ligand that the H_k protons would be diastereotopic in the dinuclear complex and that the signal would be split, confirming the helicate nature of the complex formed. However, no diastereotopic splitting of the H_k signal was observed, indicating that the ethoxy substitution is too distant from the binding sites for the chirality to have an effect that leads to observable changes of the NMR signal.

To confirm helix formation, excess of a chiral reagent was added to a solution of the [$Eu_2\mathbf{L^2}_3$] complex. Pirkle's reagent, {(S)−(+)-2,2,2-trifluoro-1-(9-anthryl)ethanol}, was chosen as the resolving reagent and has been previously employed for NMR characterization of chiral complexes.[30] Addition of Pirkle's reagent to a solution of $Eu_2\mathbf{L^2}_3$ in d^7-DMF/ d^6-acetone led to splitting of several peaks, indicating the presence of a racemic mixture in solution. The required excess of the Pirkle's reagent is probably due to the weak formation of the diastereomeric complexes due to the polar nature of the solvent. These results lead us to the conclusion that the solution structure of the complexes is indeed helical, in accordance with the previously reported dinuclear transition metal structures.[19]

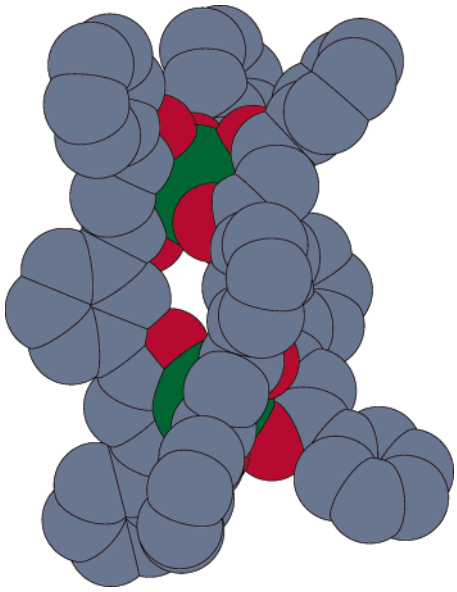

Figure 7. Molecular model of the [$Eu_2\mathbf{L^1}_3$] complex.

In the ^{1}H NMR spectrum of [$Nd_2\mathbf{L^1}_3$] in d^7-DMF a doublet at δ 10.0 with a coupling constant of J = 7.5 Hz is assigned as H_g, based on the coupling to H_h and the integration for six protons. The triplet at δ 8.28 integrates to three protons and has a ^3J of 7.5 Hz, which lead to the assignment of H_h. This resonance is not present in the spectrum of [$Nd_2\mathbf{L^2}_3$] which confirms the assignment. The remaining multiplets were assigned on the basis of integration and their likely chemical shifts: the resonance at δ 12.0 integrates for eighteen protons and is assigned to H_c and H_e. The larger multiplet at δ 8.46−8.53 integrates for twenty-one protons and is therefore assigned as H_a, H_b, and H_f. In the ^{1}H NMR spectrum of [$Nd_2\mathbf{L^2}_3$] in d^7-DMF the ethoxy peaks, H_k and H_m, are assigned unambiguously due to their coupling patterns.

The ^{1}H NMR spectrum of [$Sm_2\mathbf{L^1}_3$] in d^7- DMF exhibits a multiplet at δ 8.53−8.51, assigned to H_c and integrates correctly to twelve protons. H_g appears at δ 8.38 and the methine protons, H_e at δ 7.90. A broad singlet at δ 6.75 that integrates to three protons is assigned as H_h, although the peak is not sufficiently resolved to illustrate coupling to H_g. The remaining protons, H_a, H_b, and H_f, are accounted for by the multiplet at δ 7.56−7.50, which integrates to the correct value of twenty-one protons. The splitting pattern of this multiplet is similar to that of the

(28) Bünzli, J.-C. G., Chopin, G. R., Eds.; *Lanthanide Probes in Life and Earth Sciences*, Elsevier: Amsterdam, 1989.
(29) McConnell, H.-M.; Robertson, R. E. *J. Chem Phys.* **1958**, *29*, 1361.
(30) Chambron, J.-C.; Sauvage, J.-P.; Mislow, K.; De Cian, A.; Fischer, J. *Chem. Eur. J.* **2001**, *7*, 4086; Geraci, C.; Piatelli, M.; Neri, P. *Tetrahedron Lett.* **1996**, *37*, 7627; Zarges, W.; Hall, J.; Lehn, J. M.; Bolm, C. *Helv. Chim. Acta* **1991**, *74*, 1843.

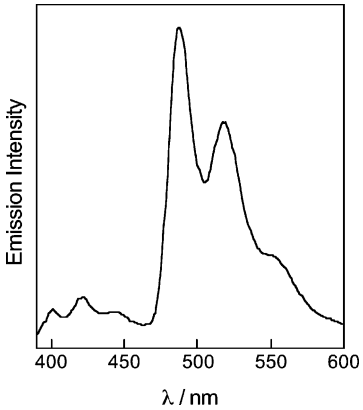

Figure 8. 77 K emission spectrum of $[Gd_2\mathbf{L^1}_3]$ in DMF:MeOH, 1:4 $\lambda_{exc} = 368$ nm.

multiplets observed in the ^{1}H NMR spectra of $[Nd_2\mathbf{L^1}_3]$ and $[Nd_2\mathbf{L^2}_3]$, which are, unambiguously assigned also, to protons H_a, H_b, and H_f. This fact provides further validation of our assignment.

In light of the mass spectral and NMR data, the lanthanide complexes $[M_2\mathbf{L^1}_3]$ and $[M_2\mathbf{L^2}_3]$ may be represented with molecular models as neutral triple stranded dinuclear lanthanide helices (Figure 7). The construction of the models was performed using MM2 calculations based on the $H_2\mathbf{L^1}$ ligand crystal structure and the reported structures for the transition metal complexes of $H_2\mathbf{L^1}$.[19] In the models, no solvent molecules were considered. Many of the tris-diketonate complexes of lanthanides are 8-coordinate in the solid state, with solvent molecules filling the six-coordinate lanthanide coordination sphere.[31] The number of coordinated solvent molecules can be determined, under certain conditions, using time-resolved luminescence spectroscopy and this approach is used in a later section.

Luminescence Properties of Triple Stranded Dinuclear Complexes of $\mathbf{L^1}$ and $\mathbf{L^2}$. Properties of $\mathbf{L^1}$ and $\mathbf{L^2}$ as Sensitizers for Lanthanide Emission. To investigate the photophysical properties of the energy donor $\pi\pi^*$ state of the ligand we examined the luminescence properties of the Y(III) and Gd(III) complexes. The room-temperature emission spectrum of a degassed DMF solution of $[Y_2\mathbf{L^1}_3]$ exhibits a broad emission band with $\lambda_{max} = 436$ nm, attributable to a ligand $\pi^* \rightarrow \pi$ transition (Supplementary Info). The ligand phosphorescence is clearly observed in the 77 K emission spectrum of the $[Gd_2\mathbf{L^1}_3]$ complex (Figure 8).

As the energy of the ligand-centered triplet state does not depend significantly on the metal, measurement of the short-wavelength, 0−0 transition of $[Gd_2\mathbf{L^1}_3]$ gives the energy of the $^3\pi\pi^*$ level for all the lanthanide chelates of $\mathbf{L^1}$. The 0−0 transition in this case is the band at 490 nm (20408 cm^{-1}). The vibrational progression of 1300 cm^{-1} may be assigned to either C−C or C−O stretching frequencies.[31,32] The energy of this state is higher than the emitting excited states of Eu(III), Sm(III), and Nd(III) confirming the suitability of the ligand as a sensitizer for those lanthanides (Figure 9). However, this ligand is not suitable for Tb(III) and Dy(III) which possess higher energy excited states.

Red and Pink Luminescent Complexes Based on Eu(III) and Sm(III). Light excitation into the ligand $^1\pi\pi^*$ state at 350 nm of $[Eu_2\mathbf{L^1}_3]$ in DMF or MeOH is followed by strong red luminescence, characteristic of the $^5D_0 \rightarrow {}^7F_J$ ($J = 0-4$) emission bands of Eu^{3+} (Figure 10). Although the resolution of these spectra precludes a detailed analysis of the symmetry of the complexes, the similarity of the structured emission patterns in both solvents suggests that there are no solvent-dependent structural changes.

The excitation spectrum of $[Eu_2\mathbf{L^1}_3]$ has a band maximum at around 360 nm, which matches the corresponding absorption spectrum, confirming that energy transfer takes place from the ligand to the Eu(III) ion. (Figure 11). The $[Eu_2\mathbf{L^2}_3]$ complex showed similar emission and excitation spectra as the $\mathbf{L^1}$ analogue. The $\pi \rightarrow \pi^*$ bands at $\lambda_{max} = 357$ nm in the absorption spectra of all complexes have extinction coefficients of $\epsilon = 13$

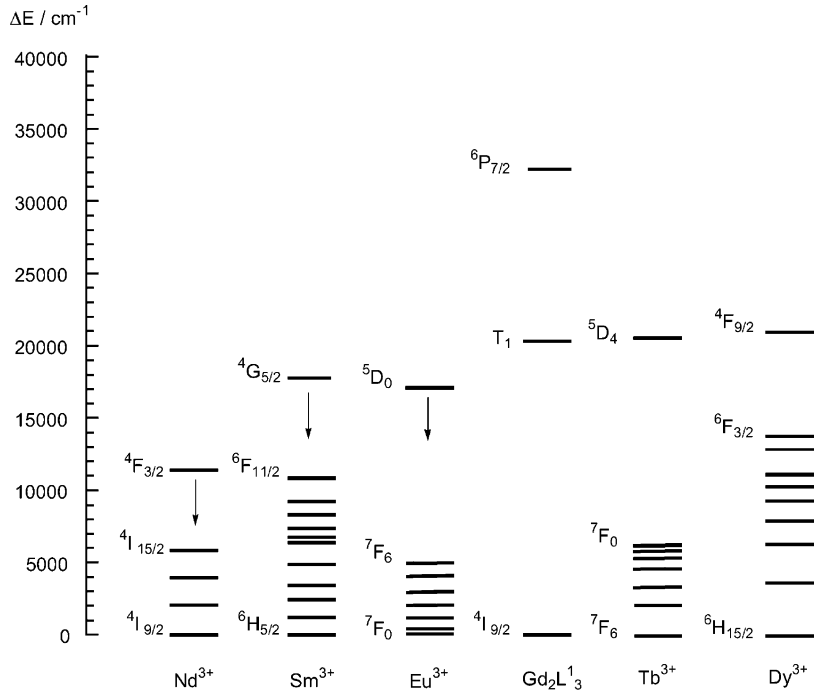

Figure 9. Simplified energy diagram showing the lowest lanthanide excited states and the estimated triplet state of the sensitizer $\mathbf{L^1}$ in the $[Gd_2\mathbf{L^1}_3]$ complex.

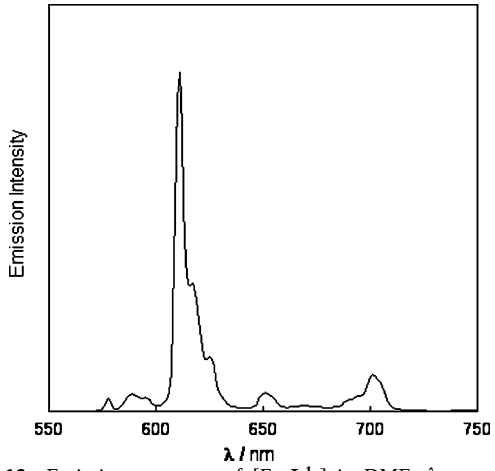

Figure 10. Emission spectrum of $[Eu_2\mathbf{L^1}_3]$ in DMF, $\lambda_{exc} = 350$ nm, corrected for PMT response.

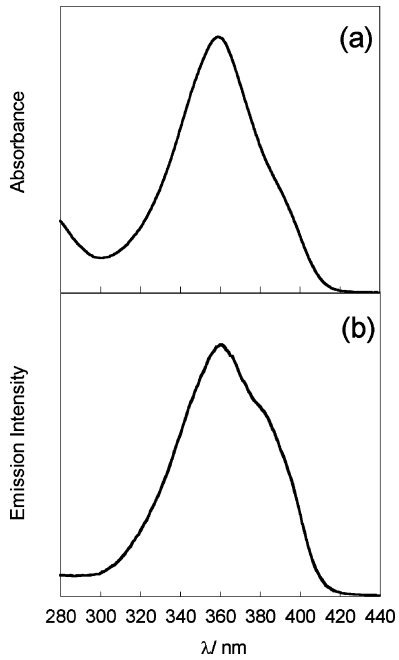

Figure 11. Absorption (a) and excitation (b) spectra of $[Eu_2\mathbf{L^1}_3]$ in DMF. The excitation spectrum was corrected for lamp and instrument response; the luminescence signal was monitored at $\lambda_{em} = 610$ nm.

$\times 10^4$ dm^3 mol^{-1} cm^{-1} that confirm the presence of three ligands per complex in solution.

The luminescence lifetimes of $[Eu_2\mathbf{L^1}_3]$ in DMF, MeOH, and MeOD were measured at room temperature (RT) and 77 K (Table 1), following excitation into ligand-centered bands ($\lambda_{exc} = 355$ nm).

Each of the measured luminescence decays is described by monoexponential kinetics, even at 77 K, and this suggests that both Eu^{3+} ions have the same environment in the complex. This agrees with the high symmetry observed in the NMR spectra of all the complexes.

It is clear from Table 1 that there is a pronounced variation in the $^5D_0$ luminescence decay with solvent. This trend can be partly rationalized in terms of the vibrational quenching effect of coordinated solvent molecules. The lifetime is longer in MeOD than in MeOH due to the replacement of the high-energy O−H oscillators with low-energy O−D oscillators. In DMF, the measured lifetimes are probably affected by traces of water, which coordinate to the metal ion since DMF was not dried prior to use. The measurement of lifetimes in both MeOH and MeOD allows an estimation of the number of coordinated solvent molecules (q) (equation 1)[33]

Table 1. Luminescence Lifetimes of the Eu^{3+} ($^5D_0$) Level in $[Eu_2L^1_3]$ ($\lambda_{exc} = 355$ nm)

solvent	τ (RT)/ms	τ (77 K)/ms
DMF	0.22	0.46
MeOH	0.20	0.35
MeOD	0.30	0.65

$$q = A(1/\tau_{MeOH} - 1/\tau_{MeOD} - a) \quad (1)$$

where A is a proportionality constant for a given ion a is a correction factor for outer sphere molecules and the lifetimes are given in ms. In this equation, we have modified the previously used methods for coordinated methanol molecules rather than coordinated water.[33a] Application of eq 1 to the values given in Table 1, gives the values $q = 3.7$ and 2.9 at RT and 77 K respectively when $a = 0.125$ and $A = 2.4$ for Eu^{3+} in MeOH.[33b] However, this method is optimized for $q = 1$ and if we use the latest modified approach[33c] that takes into account $q > 1$ with $a = 0.15$ and A = 2.2 in eq 1 this leads to q values of 3.4 and 2.6 at RT and 77 K, respectively. Within experimental error, this is good evidence that for $[Eu_2\mathbf{L^1}_3]$ in methanol there are three solvent molecules coordinated to each Eu^{3+} ion, giving the Eu^{3+} ions the common solution coordination number of nine. In addition to a solvent-dependence, the $^5D_0$ luminescence lifetime increases dramatically with a decrease in temperature from room temperature to 77 K in each of the three solvents. The overall luminescence decay rate constant, k, can be expressed by eq 2

$$k = k_r + k_{nr}(T) + k_{nr}(OH) + k_{nr}(\text{other vibr.}) \quad (2)$$

where k_r is the radiative rate constant, $k_{nr}(T)$ is the nonradiative temperature-dependent rate constant, $k_{nr}(OH)$ is the nonradiative temperature-independent rate constant due to O−H oscillators and k_{nr}(other vibr.) is the same rate constant for vibrations other than O−H.[5e] The values of these constants can be obtained for $[Eu_2\mathbf{L^1}_3]$ from the measurements made in MeOH and MeOD if the following assumptions are made: k_{nr}(other vibr.) is negligible (there is only one other nearby C−H oscillator per ligand, and the effect of C−H is small[33] in distances of >4 Å), coupling with O−D oscillators is inefficient and at 77 K thermally activated processes do not operate. It follows that

$$k_r = 1/\tau(77\text{ K, OD}) \quad (3)$$

$$k_{nr}(RT) = 1/\tau(RT, OD) - 1/\tau(RT, OD) \quad (4)$$

$$k_{nr}(OH) = 1/\tau(RT, OH) - 1/\tau(RT, OD) \quad (5)$$

Calculations for $[Eu_2\mathbf{L^1}_3]$ using eqs 3−5 give values of 1500 s^{-1}, 1800 s^{-1} and 1700 s^{-1} for k_r, $k_{nr}(RT)$ and $k_{nr}(OH)$, respectively. The term $k_{nr}(OH)$ is the same as that used to calculate the number of coordinated solvent molecules in eq 1,

(31) Whan, R. E.; Crosby, G. A. *J. Mol. Spectroscopy* **1962**, *8*, 315.
(32) Sager, W. F.; Filipesen, N.; Serafin, F. A. *J. Phys. Chem.* **1965**, *69*, 1092.
(33) (a) Holz, R. C.; Chang, C. A.; Horrocks, W. D., Jr. *Inorg. Chem.* **1991**, *30*, 3270. (b) Beeby, A.; Clarkson, I. M.; Dickins, R. S.; Faulkner, S.; Parker, D.; Royle, L.; De Sousa, A. S.; Williams, J. A. G.; Woods, M. *J. Chem. Soc., Perkin Trans. 2* **1999**, 493. (c) Supkowski, R. M.; Horrocks, W. D., Jr. *Inorg. Chem.* **1999**, *38*, 5616.

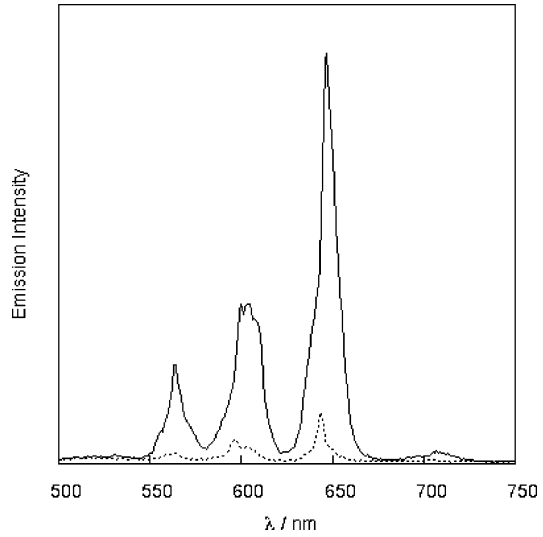

Figure 12. Emission spectra of isoabsorptive solutions (A = 0.1) of $[Sm_2\mathbf{L^1}_3]$ (solid line) and $[Sm(DBM)_3]$ (dotted line) in DMF, $\lambda_{exc} = 353$ nm.

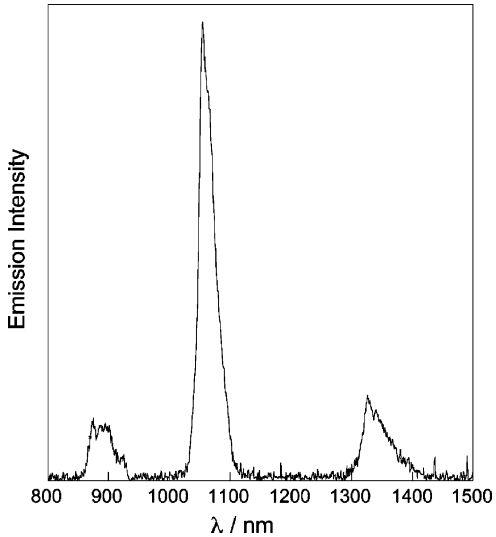

Figure 13. Emission spectrum of $[Nd_2\mathbf{L^1}_3]$ in d^7-DMF, $\lambda_{exc} = 358$ nm.

and the value of 1700 s^{-1} is indicative of an efficient nonradiative pathway.

The temperature-dependent rate constant, $k_{nr}(T)$, plays a role when short-lived, higher-energy states are thermally accessible, and in this instance, the calculated value of 1800 s^{-1} for k_{nr}(RT) is significant. A common deactivation process encountered in lanthanide complexes is the back transfer of energy from the metal excited state to the ligand triplet state. From the phosphorescence data, the triplet state is around 3000 cm^{-1} above the $^5D_0$ level of Eu^{3+}. This gap is too large, however, to allow the reverse process. This is confirmed by the lack of any changes in lifetime following deaeration of a DMF solution of $[Eu_2\mathbf{L^1}_3]$ with oxygen-free dinitrogen. We suggest, therefore, that the thermal quenching of the $^5D_0$ level of Eu^{3+} in $[Eu_2\mathbf{L^1}_3]$ occurs by a LMCT process. It is not uncommon for the luminescence decay of europium β-diketonates to be strongly temperature dependent and this has been previously attributed to a ligand to metal charge transfer state.[34]

In addition to the time-resolved measurements, the luminescence quantum yield of $[Eu_2\mathbf{L^1}_3]$ in DMF at room temperature was measured to be 5%. The lifetime and quantum yield of $[Eu_2\mathbf{L^2}_3]$ are similar to that of the $\mathbf{L^1}$ complex, which indicates that the ligand substitution in $\mathbf{L^2}$ does not affect the lanthanide coordination sphere. The quantum yields of $[Eu_2\mathbf{L^1}_3]$ and $[Eu_2\mathbf{L^1}_3]$ are higher than the ones reported for $[Eu(DBM)_3]$,[35] which we attribute to the effect of an additional Eu^{3+} lumophore in the dinuclear complexes, since the triplet state differences are not significant. The energy of the $\mathbf{L^1}$ state is around 200 cm^{-1} lower than the one of HDBM, which is not significantly different to affect the energy transfer.

The suitability of the ligand as a sensitizer for Sm(III) luminescence was examined. Excitation of $[Sm_2\mathbf{L^1}_3]$ solutions at 350 nm leads to strong pink emission of Sm^{3+} due to $^4G_{5/2} \rightarrow {}^6H_J$ (J = 5/2, 7/2, 9/2, 11/2) transitions; the most intense peak is the hypersensitive transition $^4G_{5/2} \rightarrow {}^6H_{9/2}$ at 647 nm (Figure 12). The quantum yield of $[Sm_2\mathbf{L^1}_3]$ was measured to be 0.16% and its lifetime in DMF was found to be 13 μs. The value of quantum yield indicates that the ligand acts as a good sensitizer for Sm(III). Sm(III) complexes are known to have weak luminescence with the main source for nonradiative loss attributed to multiphonon emission.[36] Ligand to metal charge-transfer transitions are higher in energy than those present in the relevant Eu(III) complexes, hence they do not lead to significant energy loss via radiationless quenching. The observed luminescence lifetime is longer than the reported value of $[Sm \subset 2.2.1]^{3+}$ in water (5 μs) where the Sm(III) is hexacoordinate. The value is slightly shorter than the reported values of nonacoordinated complexes (around 40 μs)[37] possibly due to the fact that there may be up to three water molecules coordinated to Sm(III), since no special care was taken for drying the DMF solvent. Indeed, most of the studies for Sm(III) are performed in dry or deuterated solvents to minimize the effect of O−H and C−H deactivation pathways.[7a]

To examine the effect of the second lanthanide ion we performed a luminescence quantum yield experiment to compare the luminescence signal intensity between $[Sm(DBM)_3]$ and $[Sm_2\mathbf{L^1}_3]$. The luminescence signals of isoabsorptive solutions of the two complexes were examined under quantum yield conditions (Figure 12). Comparison of the integrated luminescence signals of the two complexes shows that the dinuclear complex displayed 11 times higher signal intensity than the mononuclear complex. This confirms the effect of the second lumophore in the increase of the luminescence signal, and it is in agreement with the results of the europium complex. This increase in quantum yield is particularly important for samarium complexes that are weaker emitters.

Near-IR Emitting Nd(III) Complexes. The $[Nd_2\mathbf{L^1}_3]$ complex is found to be luminescent, as expected based on the energy level of the triplet state which is higher than the Nd luminescent excited state, $^4F_{3/2}$ (11 527 cm^{-1}). Excitation of the ligand absorption band of $[Nd_2\mathbf{L^1}_3]$ at 358 nm resulted in narrow band emission at 890, 1054, and 1325 nm (Figure 13). The emission bands were assigned to $^4F_{3/2} \rightarrow {}^4I_{9/2}$, $^4I_{11/2}$ and $^4I_{13/2}$ transitions, respectively. The experiment was performed in d^7-DMF to avoid

(34) Berry, M. T.; May, P. S.; Xu, H. *J. Phys. Chem.* **1996**, *100*, 9216.
(35) Dawson, W. R.; Kropp, J. L.; Windsor, M. W. *J. Chem Phys.* **1966**, *45*, 2410.
(36) Sabbatini, N.; Dellonte, S.; Blasse, G. *Chem. Phys. Lett.* **1986**, *129*, 541.
(37) e Silva, F. R. G.; Malta, O. L.; Reinhard, C.; Gudel, H. U.; Piguet, C.; Moser, J. E.; Bunzli, J. C. G. *J. Phys. Chem. A* **2002**, *106*, 1670.

quenching by C−H vibration (5900 cm^{-1}, $\nu = 2$) of the lowest in energy Nd(III) band $^4F_{3/2} \rightarrow {}^4I_{15/2}$ (5400 cm^{-1}).

Time-resolved experiments were also performed by excitation of a d^7-DMF solution of $[Nd_2\mathbf{L^1}_3]$, and monitoring the decay of the emission of the strongest emission band at 1054 nm. Analysis of the monoexponential decay results in a lifetime of 1.5 μs. This value compares well with the reported lifetime of the tris(hexafluoroacetylacetonato) Nd(III) complex in DMF,[38] indicating that the bond vibrations in the $\mathbf{L^1}$ ligand do not efficiently quench the excited state of Nd(III). The reasons for this are 3-fold; (a) in $Nd_2\mathbf{L^1}_3$ there are few C−H bonds in close proximity to the metal ion; (b) the closest *o*-protons of the phenyl rings are estimated to be located at distances of over 4 Å (estimated from model, Figure 7) with the exception of the H_f proton on the central 1,3-substituted phenyl ring; (c) the C−H aromatic vibration is usually slightly higher (3050−3100 cm^{-1}) than the aliphatic C−H vibration leading to a poorer match of the vibrational levels responsible for luminescence signal deactivation.

In other reported Nd complexes, the ligand design to maximize luminescence lifetime is based on either podand,[39] macrocylic[40] or fluorinated diketonate structures[41] which lead to complexes with similar lifetime values as in our case. An exception is the perfluoro sulfonylamine ligands that yield complexes with longer Nd(III) lifetimes.[42]

An estimated quantum yield of Nd(III) luminescence of a certain complex may be calculated by comparison of the luminescence lifetime of the complexed ion[43] with the natural lifetime of Nd, τ_0. By using eq 6 a value of 0.6% for the quantum yield of the complex is calculated, given a value, τ_0, for the natural lifetime of Nd(III) = 270 μs.[44]

$$\Phi = \tau/\tau_0 \qquad (6)$$

This method of quantum yield estimation does not take into account other factors such as intersystem crossing efficiency of absolute quantum yield methods using standards. The obtained quantum yield value compares very well with other Nd(III) complexes where all the protons of the ligands are either deuteurated or fluorinated, e.g., the Nd(III) complex of hexafluoroacetylacetonate[41] is reported to have a quantum yield of 0.3%. These results indicate again that most of the C−H vibrations are not in close proximity to the lanthanide center, which indicates that these bis diketonate ligands are ideal sensitizers for near-IR luminescence.

Quadruple-Stranded Dinuclear Complexes of $\mathbf{L^1}$, $(Hpip)_2[Eu_2\mathbf{L^1}_4]$. Although the formation of mononuclear tetrakis diketonate complexes has been previously examined in the solid state and their X-ray crystal structures have been determined,[45] tetrastranded dinuclear lanthanide complexes have not previously been investigated. The tetrakis- $\mathbf{L^1}$ complex of Eu^{3+} was prepared by altering the ligand-to-metal ratio to 2:1 and using piperidine to act as counterion. Electrospray mass spectrometric analysis of freshly prepared solutions of $(Hpip)_2[Eu_2\mathbf{L^1}_4]$ showed a peak for the doubly charged species $[Eu_2\mathbf{L^1}_4]^{2-}$, confirming the formulation of the complex (Figure 14).

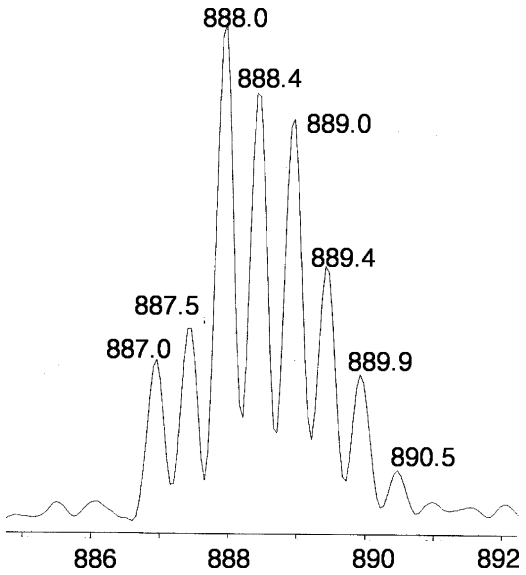

Figure 14. Expanded region of the ES−MS(−) spectrum of $(Hpip)_2[Eu_2\mathbf{L^1}_4]$ displaying the peak of the doubly charged species $[Eu_2\mathbf{L^1}_4]^{2-}$.

The luminescence spectrum of the powder of $(Hpip)_2[Eu_2\mathbf{L^1}_4]$ showed some notably different features when compared with the spectrum of the $[Eu_2\mathbf{L^1}_3]$ powder (Figure 15). First, the Eu^{3+} luminescence, following UV irradiation, is much stronger for the tetrakis complex, as expected due to the absence of any coordinated solvent molecules. Second, the fine structure of the hypersensitive $^5D_0 \rightarrow {}^7F_2$ emission band is clearly different in both cases. This indicates that the symmetry around the europium ions in the two complexes is not the same, as anticipated for a tris- vs tetrakis-complex.[46] The higher the symmetry the less splitting is observed for the $^5D_0 \rightarrow {}^7F_2$ band. Taking into account the resolution limits of our instrument, we can conclude that the tetrakis complex appears to have higher symmetry than the tris, attributed to the lack of solvent molecules coordinated to the Eu(III) ion and the additional ligand. The Y(III) tetrakis-complex was also prepared to examine the NMR spectroscopic features. The NMR spectrum showed overlapping peaks rather than the simple pattern observed in the tris complexes, indicating the presence of an equilibrium between the two species in solution. This is not surprising since ligand dissociation in solution can readily take place leading to formation of the tris-species which may be affected by the polarity of the solvent and the concentration of the sample. Attempts to crystallize dinuclear tetrakis complexes were unsuccessful.

(38) Hasegawa, Y.; Kimura, H.; Murakoshi, K.; Wada, Y.; Kim, J. H.; Nakashima, N.; Yamanaka, T.; Yanagida, S. *J. Phys. Chem.* **1996**, *100*, 10201.
(39) Oude Wolbers, M. P.; van Veggel, F. C. J. M.; Peters, F. G. A.; van Beelen, E. S. E.; Hofstraat, J. W.; Geurts, F. A. J.; Reinhoudt, D. N. *Chem. Eur. J.* **1998**, *4*, 773.
(40) Faulkner, S.; Beeby, A.; Carrie, M.-C.; Dadabhoy, A.; Kenwright, A. M.; Sammes, P. G. *Inorg. Chem. Commun.* **2001**, *4*, 187; Faulkner, S.; Beeby, A.; Dickins, R. S.; Parker, D.; Williams, J. A. G. *J. Fluoresc.* **1999**, *9*, 45.
(41) Yanagida, S.; Hasegawa, Y.; Murakoshi, K.; Wada, Y.; Nakashima, N.; Yamanaka, T. *Coord. Chem. Rev.* **1998**, *171*, 461.
(42) Hasegawa, Y.; Ohkubo, T.; Sogabe, K.; Kawamura, Y.; Wada, Y.; Nakashima, N.; Yanagida, S. *Angew. Chem., Int. Ed.* **2000**, *112*, 365.
(43) Klink, S. I.; Hebbink, G. A.; Grave, L.; Peters, F. G. A.; Van Veggel, F. C. J. M.; Reinhoudt, D. N.; Hofstraat, J. W. *Eur. J. Org. Chem.* **2000**, 1923.
(44) Weber *Phys. Rev.* **1968**, *171*, 283.
(45) Sweeting, L. M.; Rheingold, A. L. *J. Am. Chem. Soc.* **1987**, *109*, 2652; Rheingold, A. L.; King, W. *Inorg. Chem.* **1989**, *28*, 1715.
(46) Brecher, C.; Samelson, H.; Lempicki, A. *J. Chem. Phys.* **1965**, *42*, 1081; Bauer, H.; Blanc, J.; Ross, D. L. **1965**, *42*, 1599; Horrocks, W. D., Jr.; Albin, M. *Progr. Inorg. Chem.* **1983**, *31*, 1.

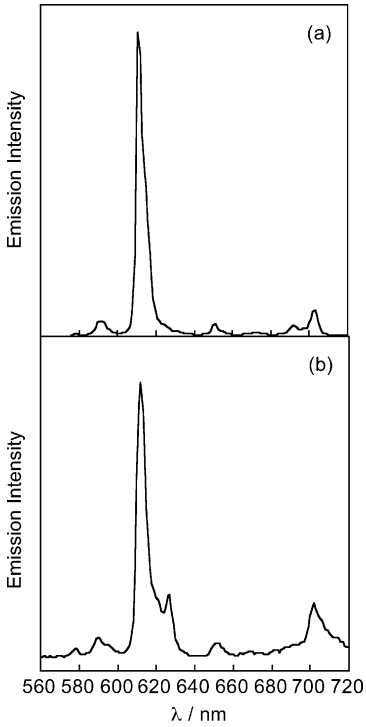

Figure 15. Emission spectra of powder samples of (a) $(Hpip)_2[Eu_2\mathbf{L^1}_4]$ (b) $[Eu_2\mathbf{L^1}_3]$, λ_{exc} = 350 nm, 2 nm band-pass (em.), corrected for PMT response.

Conclusions

The results of this work represent a novel ligand design based on diketonate binding units for the assembly of neutral tris- and quadruple-stranded dinuclear lanthanide complexes with interesting luminescent properties. NMR spectroscopy has been used to fully assign the proton environments for paramagnetic lanthanide and diamagnetic analogue complexes. Addition of Pirkle's reagent to solutions of the tris stranded complexes allows the identification of complex chirality. The sensitizing properties of the ligands have been investigated by luminescence spectroscopy. The ligand $^3\pi\pi^*$ state is well placed to allow energy transfer to Eu^{3+}, Sm^{3+} and Nd^{3+} excited states, following UV absorption. The complexes have long luminescence lifetimes and high luminescence quantum yields, even in the case of the Eu^{3+} complex where it is shown that the presence of a thermally activated LMCT pathway acts to deactivate the $^5D_0$ state. These results indicate that the energy transfer process is efficient. Internuclear cross relaxation and energy migration pathways may be operational in di- or poly- nuclear lanthanide complexes. However, in our systems the magnitude of the lifetimes and the luminescence efficiency of the dinuclear complexes as compared with the mononuclear species indicate that such processes do not contribute significantly to luminescence quenching. The ligand does not possess well-matched C−H vibrations that can quench the lanthanide excited state. This ligand feature is particularly important in the design of the near-IR emitting lanthanide complexes. The only closely spaced oscillators for vibrational quenching are the O−H oscillators attributed to the three water or methanol molecules bound to each lanthanide due to the hexacoordinate nature of the metal environment. These oscillators are excluded in the formation of the quadruple-stranded complexes where a fourth ligand replaces the coordinated solvent molecules. Quadruple-stranded dinuclear europium complexes have been isolated in the solid state and they display strong luminescent properties. The tetrakis complexes display stronger luminescent signals than the tris-complexes and have a distinct luminescence pattern. The synthetic versatility of these binucleating ligands allows an interesting and diverse array of dinuclear complexes to be synthesized to give strong emitters in the visible and near-infrared.

Acknowledgment. We acknowledge the support of EPSRC, BBSRC, and the Royal Society exchange program for funding as well as CCLRC and Simon Teat for time in the synchrotron radiation laboratory.

Supporting Information Available: The crystal structure of $H_2\mathbf{L^1}$; $^1H-^1H$ COSY spectrum of $H_2\mathbf{L}^1$; MALDI-MS and accurate FABMS spectra of the complexes; ^1H NMR spectrum of $H_2\mathbf{L^2}$; ^{13}C NMR spectra; ^1H NMR spectra of all complexes. This material is available free of charge via the Internet at http://pubs.acs.org.

JA048022Z